ResearchGate

See discussions, stats, and author profiles for this publication at: https://www.researchgate.net/publication/365928633

NDNN based U-Net: An Innovative 3D Brain Tumor Segmentation Method

Conference Paper · October 2022

DOI: 10.1109/UEMCON54665.2022.9965705

CITATIONS
12

READS
110

3 authors:

Sandeep Trivedi

25 PUBLICATIONS **141** CITATIONS

SEE PROFILE

Nikhil Patel

15 PUBLICATIONS **110** CITATIONS

SEE PROFILE

Nuruzzaman Faruqui

Daffodil International University

28 PUBLICATIONS **257** CITATIONS

SEE PROFILE

All content following this page was uploaded by Nuruzzaman Faruqui on 03 May 2023.

The user has requested enhancement of the downloaded file.

NDNN based U-Net: An Innovative 3D Brain Tumor Segmentation Method

Sandeep Trivedi
Deloitte Consulting LLP,
Houston, United States of America
Email: sandeeptrivedi@ieee.org
ORCID: 0000-0002-1709-247X

Nikhil Patel
University of Dubuque,
Iowa, United States of America
Email: patelnikhilr88@gmail.com
ORCID: 0000-0001-6221-3843

Nuruzzaman Faruqui
Department of Software Engineering,
Daffodil International University,
Daffodil Smart City, Dhaka,
Bangladesh
Email: faruqui.swe@diu.edu.bd
ORCID: 0000-0001-9306-9637

***Abstract*—Identifying and segmenting brain tumors using multi-sequence 3D volumetric MRI scans is time-consuming and challenging. Deep learning-based automatic image segmentation approaches are promising solutions to segment brain tumors from MRI 3D reconstructed images. However, T1, T1c, T2, and FLAIR modalities, along with High Graded Gliomas (HGG) and Low Graded Gliomas (LGG), make automatic brain tumor segmentation using deep learning a challenging task. A novel Nested Deep Neural Network (NDNN) has been designed, implemented, and experimented with in this paper, along with an innovative Multimodality Fusion Network (MFS Net). The proposed network segments brain tumors from 3D volumetric images and imposes the extracted feature map on the 3D region with 90.02%, 85.11%, and 85.41% dice score for Whole Tumor (WT), Core Tumor (CT), and Enhancing Tumor (ET) respectively. The novel architecture, innovative multimodality fusion, and outstanding performance of the proposed methodology have been studied, demonstrated, and compared in this paper.**

Keywords—Brain Tumor Segmentation, 3D Images, Multimodalities Fusion, 3D U-Net, Nested DNN

I. INTRODUCTION

The computer-aided automatic medical image segmentation and classification have added a new dimension to the biomedical engineering and healthcare sector. The advancement in Deep Learning has enabled the implementation of human-like intelligence in diagnosis, which is often challenging because of the lack of resources, difficulty accessing proper healthcare facilities, and the nature of the reports. Employing deep learning-based human-like intelligence to automate such diagnosis is a promising field of research as it is a potential solution to numerous problems related to the healthcare sector. Brain tumor segmentation is one of them. Functionalities and anomalies related to the brain are crucial for any living being. It is essential to analyze 3D brain images to segment brain tumors because the shape, volume, and depth are important to diagnose and prescribe appropriate treatment [1].

The 3D MRI of the brain is recorded in multimodalities. Different modality contains different type of information.

That is why it is essential to consider all modalities while diagnosing brain tumors. Analyzing every modal, merging various factors belonging to these modalities, and diagnosing the appropriate state of the tumor is a time-consuming and challenging task [2]. Computer-aided systems to fuse multimodalities of MRI scans into a single 3D volumetric image which preserves the information of every modal but minimizes the complexities of multimodal is a promising solution to biomedical engineering. Numerous approaches have been developed and experimented with acceptable results [3]. However, different methods with multiple tuning parameters dependent on numerous variables lead to multimodality fusion in different directions, from where it is challenging to discover an optimized way or the way to optimize a particular solution [4]. A deep neural

Network efficiently designed for multimodality fusion dramatically reduces the operational and optimization complexities.

Brain tumors are alarming for patients and their families [5]. Proper treatment assisted by advanced equipment is available nowadays [6]. However, nothing can be helpful unless the brain tumor is diagnosed correctly. Early diagnosis and detection of brain tumors help save lives [7]. Multiple factors are associated with the early diagnosis of brain tumors, including access to proper diagnostic centers, experienced and expert radiologists, tumor features, and the tumor's effect on a patient's health and daily life. Here the roles of the radiologists are crucial. Advanced technology and imaging devices are used to scan the brain. The radiologists who perform the diagnosis. Without any doubt, the quality of the diagnosis depends on radiologists' experience and expertise. Using computer-aided deep learning-based automatic diagnosis systems is promising in significantly reducing the burdens of radiologists, improving the quality of diagnosis, and consequently reducing the mortality rate caused by brain tumors [8]. However, the reliability and familiarity of such systems are yet to reach an acceptable level. Improving the performance of the deep learning-based brain tumor segmentation process contributes to the adaption of automatic brain tumor segmentation using deep learning technology in the applied medical sector.

This paper has addressed the research gap and scope of multimodal fusion to single voxel and innovated new deep neural networks to improve the dice score in prediction. The experiment developed and presented in this paper contributes in:

- Multimodal image fusion using a simplified inception network for brain tumor MRI modalities fusion.
- Development of a novel Nested Deep Neural Network inspired by the 3D U-Net architecture for 3D brain tumor segmentation.

The remaining part of this paper has been organized into four following sections. The related research, technological viability, and maturity have been highlighted in the second section. The third section contains the proposed methodology. The experimental results have been compared with similar research in the fourth section. Finally, the paper has been concluded in the fifth section.

II. Background

The applications of Deep Learning technology in the medical sector have started entering the mainstream instead of being confined to papers only [8]. Automatic diagnosis from MRI scans is one of these applications. The MRI contains more information and a detailed view than X-ray [11]. That is why MRI is more prevalent in medical imaging, and it has drawn considerable attention from deep learning researchers to automate diagnosis using MRI datasets [12]. In brain tumor segmentation [13], lung cancer classification [14], breast cancer classification [15], and many other diagnoses, deep learning algorithms on MRI images are demonstrating promising results in improving the quality of diagnosis. The research trends and optimistic outputs published in recent papers highlight the scope of contributing to the application of deep learning in automatic brain tumor segmentation.

MRI scans contain information recorded in modalities [16]. Different features are prominent in different modalities. That is why it is essential to use all of them while working on MRI datasets [17]. However, multimodal data processing is a complex task that can be done in multiple ways [18]. These complexities pave the path to a new scope of research, innovation, and optimization [19]. Numerous approaches have been developed to optimally process multimodal data and fuse them into a single modality. However, the scope of performance improvement and optimization to prevent data loss and effectively represent prominent information of different modalities is still an open and vibrant field of research [20]. Using an inception layer-based network for image reconstruction approach in multimodality image fusion [21] in combination with residual [22] architecture followed by sequential concatenation [23] is a promising advancement in multimodality fusion with simplified optimization options, which has been proposed in this paper.

An integrating fully convolutional neural networks (FCNNs) and Conditional Random Fields (CRFs) based framework developed in [24] demonstrates an efficient deep learning approach to segment brain tumors from the BraTS2013 and BraTS2016 datasets. However, their experiment is confined within the 2D domain, which fails to incorporate 3D volumetric features addressed in the proposed methodology. Another research published in [25] develops a deep neural network-based approach to segment brain tumors from both fully and weakly annotated. Although both 2D and 3D features have been utilized in this research, the obtained dice score for Whole Tumor (WT) and Core Tumor (CT) are 87% and 77%. The approach proposed in this paper outperforms this performance. A unique network designed in [26] significantly improves U-Net architecture brain tumor segmentation. However, this paper does not include recommended image fusion criteria which may lead to different results even after recreating the same network. Depending on the multimodality fusion process, the same network may have different results because of the modification of image features addressed in the proposed methodology.

III. Methodology

A. Image Dataset Processing

1) Dataset Description

In this research, the Brain Tumor Segmentation (BraTS) 2020 dataset has been used [27]. This dataset contains 3D volumetric MRI scans in four different modalities. These modalities are T1 weighted (T1), T1 contrast-enhanced (T1c), T2 weighted (T2), and T2 Fluid Attenuated Inversion Recovery (FLAIR). Each of these modalities is recorded at 244×244 with 155 sequences. That means the dataset comprises 3D volumetric MRI scans with $244 \times 244 \times 155$ dimensions.

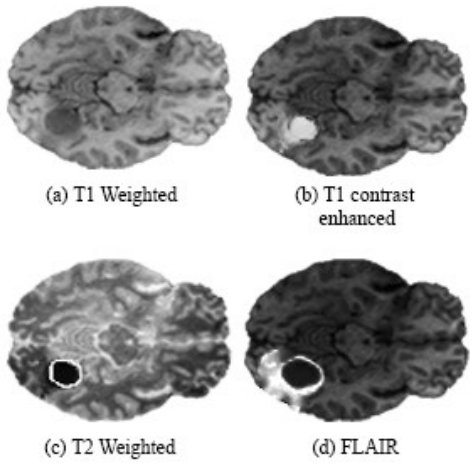

Fig. 1. An illustration of the dataset with a single MRI slice at four different modalities. Fig.1a is the T1 weighted, b is the T2 contrast-enhanced, c is T2 weighted, and d is the FLAIR modality

The goal of this experiment is to segment Whole Tumor (WT), Core Tumor (CT), and Enhancing Tumor (ET). There are five classes in the dataset. They are the background, the necrosis, the edema, the enhancing tumor, and the non-enhancing tumor. These three significant regions are constructed from the five classes available on the dataset [28, 29]. The BraTS 2020 dataset maintains the approximate ratio of WT, CT, and ET is 12:5:3. Which means 60% of the dataset contains WT. Roughly 25% of the dataset includes CT. And remaining 15% of the dataset is comprised of ET. From this approximate analysis, it has been observed that the dataset is highly imbalanced.

2) Inception Network (INet) for Data Processing

The BraTS-2020 dataset contains MRI slices recorded at four different modalities [28]. The reconstructed images used in this experiment preserve information from all modalities [30]. The accuracy of brain tumor segmentation depends on the shape, depth, and volume of the tumor. Different features are prominent in different modalities. That is why it is essential to preserve information from all possible modalities. Brain tumors are in various sizes, shapes, and volumes [31]. That is why multi-convolutions have been used instead of using single convolution. To process the data inception layer-

based network [32] named Inception Network (INet) has been developed. Figure 2 illustrates the network architecture.

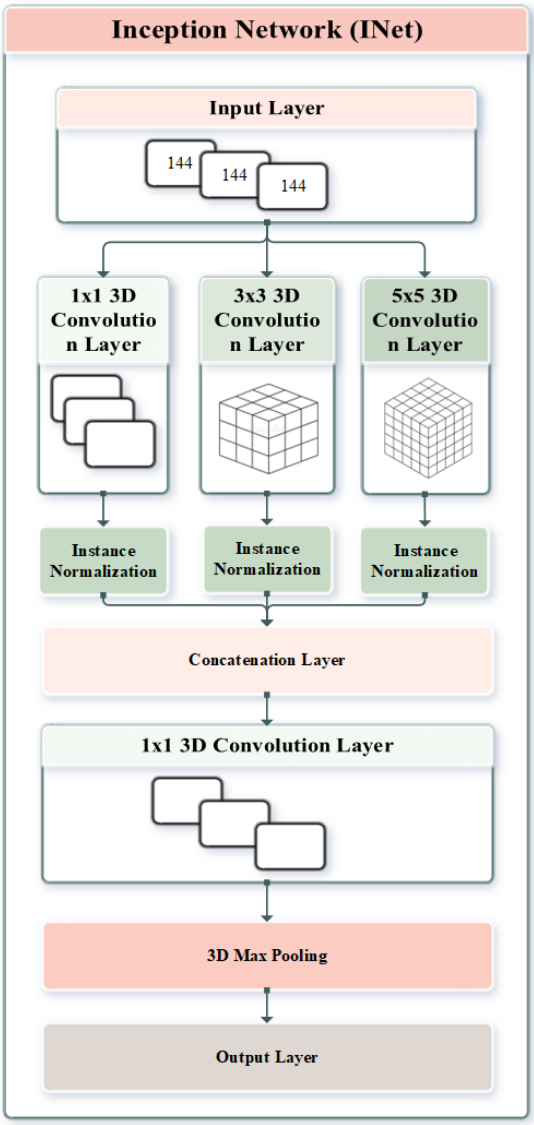

Fig. 2. The Inception Network (INet) to Process the Data

The INet consists of three types of convolutional masks - $1 \times 1, 3 \times 3$, and 5×5. Input through these masks is further processed through a 1×1 convolution kernel to merge the 3D channels into a single channel. The Rectified Linear Activation Function (ReLU) [33] has been used as the activation function of the INet, and the outputs are normalized using instance normalization layers. A concatenation layer before the 3D Max pooling layer keeps the most prominent features. Finally, the output goes to the output layer. This INet is the building block of the NDNN proposed in this paper.

3) Multimodality Fusion Net (MFS)

Using the INet, the multimodality has been fused to a single modality in this experiment. There are four modalities, T1, T1c, T2, and FLAIR, in the dataset. Each of these modalities contains valuable information related to a brain tumor. Ignoring any of these causes a loss of information. A novel Multimodality Fusion Net (MFS) has been developed and used in this experiment to perform lossless dimensionality reduction and multimodality fusion. It is illustrated in figure 3. The figure demonstrates that it is a network of INet, which, in other words, is a Nested Deep Neural Network.

The INet blocks of the first layer of MFS receive T1, T1c, T2, and FLAIR modals. This layer converts the inputs into 3D volumetric voxels. The voxels created from T1 and T1c are concatenated using a concatenation layer. The T2 and FLAIR voxels are connected too. At this level, the voxel dimension becomes $2 \times 144 \times 144 \times 144$. The outputs from the two concatenations are again transmitted to two more INet blocks. These blocks are designed to handle voxels with $2 \times 144 \times 144 \times 144$ dimensions. After that, the results of these two INets are similarly concatenated using another concatenation layer. After concatenating, the voxel dimension becomes $4 \times 144 \times 144 \times 144$. This time the 3D images contain information on all four modalities. A 3×3 convolutional layer reduces the dimension to $4 \times 48 \times 48 \times 48$. And this is the final output from the MFS Net.

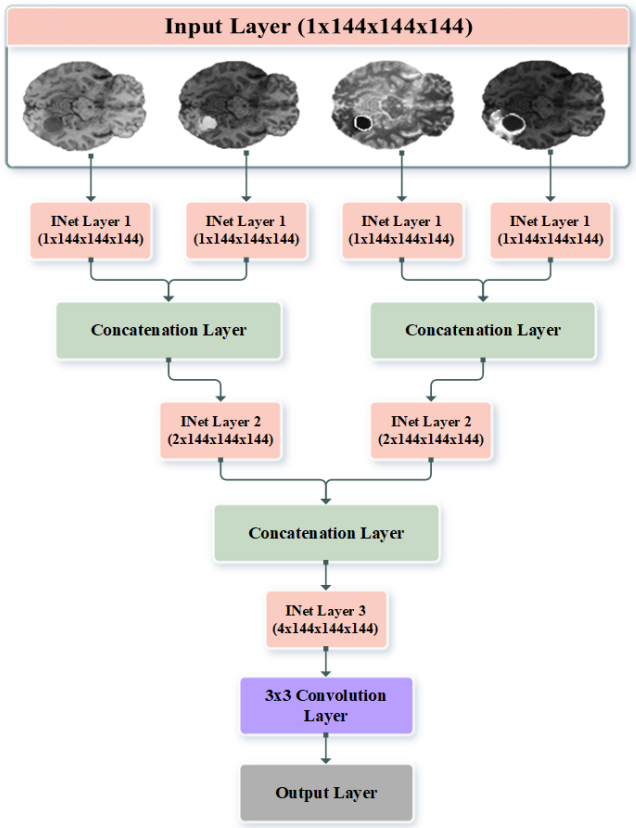

Fig. 3. Multimodality Fusion Net (MFS Net)

The output from MFS is 3D volumetric data consisting of MRI slices which preserve both spatial and depth information. At the same time, these data contain the information of all four modalities. Because of being constructed of INet, the dark MRI slices with no or nominal information are rejected during the feature learning. As a result, the ambiguous black circles from the reconstructed images disappear, which is illustrated in figure 4.

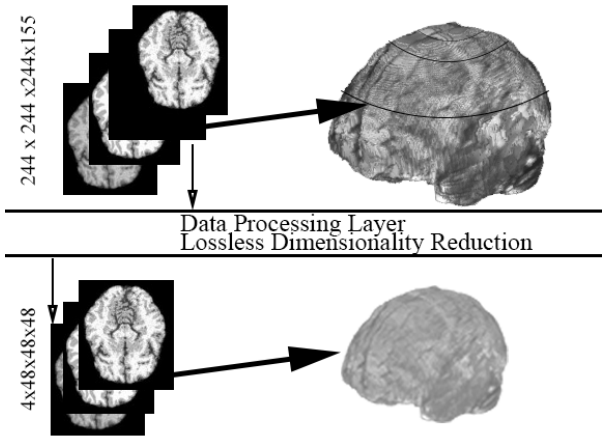

Figure 4: Output from MFS Net

The outputs from MFS Net are ready to feed into the NDNN U-Net.

B. The NDNN-based U-Net Architecture

The NDNN-based U-Net architecture is inspired by U-Net architecture [34], along with an innovative nesting of the INet block. The network consists of two parts – The Extractor and The Separator.

1) The Extractor

The Extractor extracts the brain tumor from the dimensionality-reduced image received from MFS Net. It uses the INet as a building blocks. Discovering the brain tumor pattern, locating the position of the tumor, and extracting the shape are the core functionalities of the Extractor. Unlike the MFS Net, the tumor extractor uses the Residual Network (ResNet) architecture [35]. It is illustrated in figure 5.

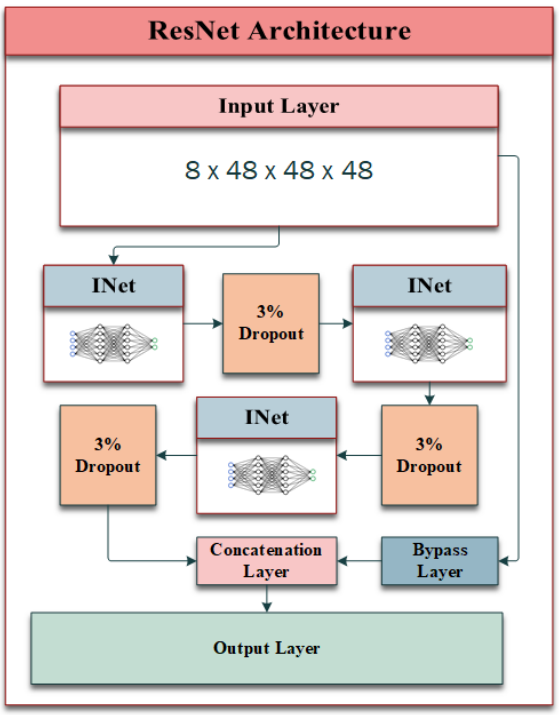

Fig. 5. The Tumor Extractor

The residual network helps prevent vanishing gradient or exploding gradient problems. At the same time, it allows skipping connection and conveys the signal of a particular layer to another layer [36]. Because of these advantages, the ResNet architecture with INet as a building block has been used as a tumor extractor.

The INet has been specially designed to fuse multimodalities into a single modality. One of the purposes of this network is to perform the lossless conversion. As a result, it emphasizes most of the features. The network tends to be overfitted with a robust correlation among features. The distributed 3% dropout layers after every INet layer prevents overfitting by weakening the correlation. After every INet layer, a 3% dropout layer has been added to prevent overfitting [37].

2) The Separator

The proposed Separator has been designed to improve the dice score. An ensemble U-Net architecture has been employed to separate the tumors from the 3D brain images. The experimental result with generic ensemble U-Net fails to generate the expected output. A Compact Node (cNode) ensemble U-Net architecture has been designed, implemented, and used in this paper to improve performance.

a) The Compact Node (cNode) Formation

The cNode consists of INet followed by a ResNet. Both of these networks have dynamic dimension processing capability. It is illustrated in figure 6.

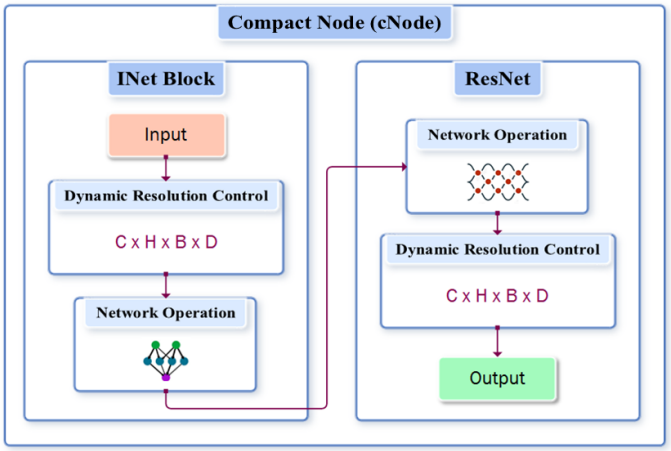

Fig. 6. Compact Node

The dimensions of the images change after processing them through INet and ResNet blocks. Using these two networks separately creates dimension-related complexity. However, when they are used as the building block of the ensemble U-Net, the different dynamic resolution imposes additional challenges. A Dynamic Resolution Control (DRC) layer has been added after the input layer of INet and before the output layer of the ResNet to tackle these challenges. The DRC keeps track of the input and output dimensions and makes these data accessible for the ensemble U-net.

b) Ensemble U-Net Architecture

The ensemble U-Net architecture illustrated in figure 7 consists of cNode, downsample, expansion, concatenation, and tensor addition node. It receives the input from the MFS Net through a cNode and a tensor addition node. After that, the signals are processed through multiple cNode and downsample nodes. The processed signals from cNode are also transmitted to the concatenation node before sampling them down. It ensures that the signal's shape, depth, and

volume are preserved. At the same time, through repeated convolution processed by the cNode, extract the features. The right chain of the U-Net expands the signal received from cNode after downsampling. In every expansion layer, the extracted but downsampled layers are upsampled and imposed on the actual volumetric signal through concatenation layers. The repetition of this process results in feature superimposes on a 3D volumetric image.

One of the drawbacks of the architecture, which has been observed during the experiment, is the overfitting problem due to the presence of numerous prominent features. As a result, the evaluation accuracy of the network drastically falls for the test dataset. This problem has been resolved by adding a 3% dropout layer in series with three cNode before sending signals processed by them to the ensemble network. The processed signals from cNode are further processed through a 1×1 convolutional layer. Then the signal is upsampled again as the convolutional layer downsamples the signals. Finally, it is concatenated with the similarly processed signal immediately next to it. After repeating it for the last three cNode, the final signals from the final expansion layer are concatenated with the cNode. This concatenated signal is processed through the Sigmoid activation function. And the final output is one of the three classes WT, CT, or ET.

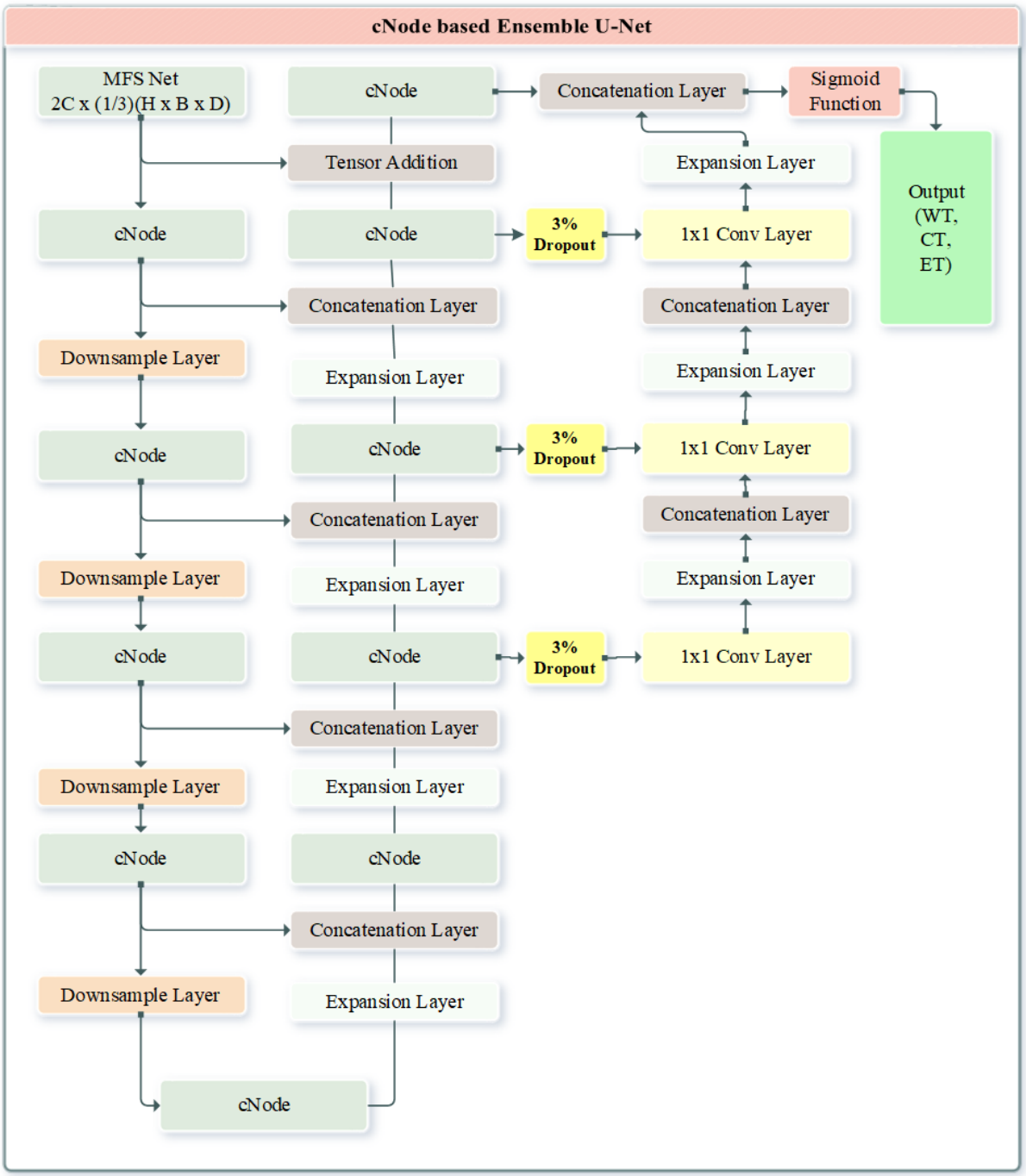

Fig. 7. The architecture of the cNode-based Ensemble 3D U-Net

IV. Experimental Results & Comparison

A. Dataset Splitting & Validation

The BraTS 2020 data set has been used to train and test the network, which is consisted of 3D volumetric MRI scans recorded in four different modalities, T1, T1c, T2, and FLAIR, with 244x244x155 dimensions. Different modalities of this dataset demonstrate different tumor features. In this experiment, scans of 150 patients were used. These data are labeled with background, necrosis, edema, enhancing tumor, and non-enhancing tumor. Based on these five labels, the three tumor regions, Whole Tumor (WT), Core Tumor (CT), and Enhancing Tumor (ET), are detected. The purpose of training the NDNN is to classify and locate the WT, CT, or ET region. The dataset has been split at a 7:3 ratio for training and testing. No other dataset has been used neither in training nor in the testing phase to restrict the experiment within the context of the BraTS2020 dataset. The k-fold cross-validation has been used at k = 5 to evaluate and optimize the network's learning process.

B. Best Optimizer Selection

Three different optimization functions at five different configurations have been experimented with in this research to ensure the optimized learning progress and best performance. The training loss and validation error for RMSProp [38], Adam at $\beta_1 = 0.9$, Adam at $\beta_1 = 1$, QHAdam at $V_1 = 0.75, \beta_1 = 0.9$, and QHAdam at $V_1 = 1, \beta_1 = 1$[39] has been illustrated in figure 8.

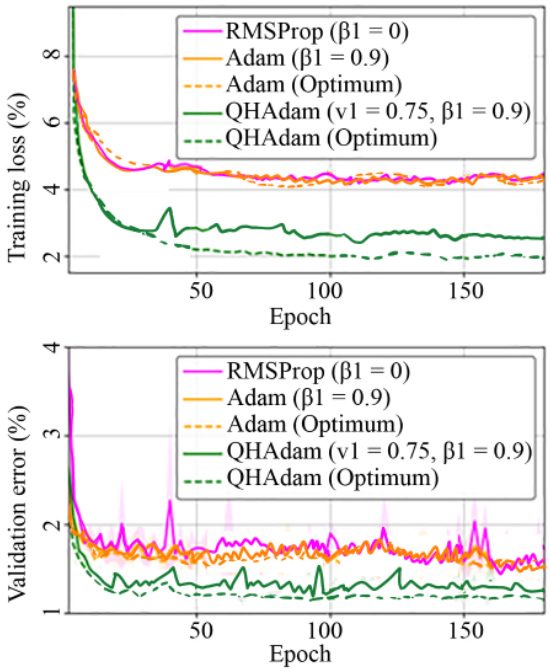

Fig. 8. The validation error and training loss for different optimizers at different configurations

According to the experimental observation, the QHAdam is the optimum performing optimizer. That is why the QHadam has been used in this paper.

C. Evaluation Metrics

The literature review suggests that the Dice Coefficient, also known as the F1-score, is a widely used evaluation metric for 3D brain tumor segmentation [40, 41, 42]. It has been defined in equation 1.

$$Dice\ coefficient = \frac{2 \times TP}{2 \times TP + FP + FN} \quad (1)$$

The Intersection-Over-Union (IOU) at Jaccard Index is another practical evaluation criterion defined by equation 2.

$$IOU = \frac{TP}{TP + FP + FN} \quad (2)$$

In Equations 1 and 2, TP, FP, and FN are the abbreviations for True Positive, False Positive, and False Negative, respectively. The classes of the BraTS2020 dataset are not evenly distributed among the dataset. As a result, the Weighted Average (WA) of IOU loss and dice loss has been used to ensure a common ground for every class. The Dice Loss (DL) is defined by equation 3.

$$DL(a, h(a)) = \left(1 - \frac{2.a.h(a)}{|a|^2 - |h(a)|^2}\right) \times 100\% \quad (3)$$

In equation 3, the a is the actual label on the dataset. The h(a) is the prediction from the network. This equation gives the dice loss on a percentage scale. The IOU Loss (IOUL) is calculated using equation 4.

$$IOUL(a, h(a)) = \left(1 - \frac{a.h(a)}{a + h(a) - ah(a)}\right) \times 100\% \quad (4)$$

The IOUL is also calculated on a percentage scale. The WA is measured using equation 5.

$$WA(a, h(a)) = 0.5\left(DL(a, h(a)) + IOUL(a, h(a))\right) \quad (5)$$

The Hausdorff95 has also been used as an evaluation criterion in this experiment [43].

D. Results & Comparison

The proposed network segments the WT, CT, and ET with 89.36%, 87.4%, and 86.33% dice scores, which are illustrated in figure 9.

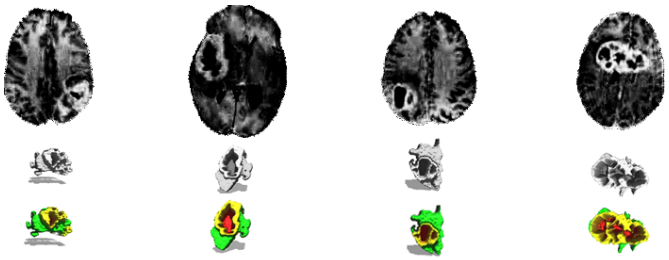

Fig. 9.: The segmented WT, CT, and ET region. The region in red is the CT. The yellow region is the ET. And the green region, including the red and yellow regions, is the WT. The tumors were segmented first, and then different colors were applied manually to identify the regions.

The network has been trained with 92.11% validation accuracy at the 200th epoch. It takes 22 minutes to complete the training. For both Adam and QHAdam, the training loss and validation loss fall rapidly for the first 28 epochs. After the 150th epoch, there are minor changes in the learning curve. However, eventually, it becomes nearly constant, and the network gets trained at the 200th epoch with 92.11% validation accuracy and 7.89% validation error. The dice score, sensitivity, specificity, and Hausdorff95 for both the training and validation phase have been tabulated in table 1.

Table 1: Performance evaluation in both training and validation phase

	Dice			Sensitivity			Specificity			Hausdorff95		
	ET	WT	TC	ET	WT	TC	ET	WT	TC	ET	WT	TC
Training	0.85	0.94	0.84	0.78	0.93	0.80	0.96	0.97	0.93	42.80	12.14	18.63
Validation	0.82	0.92	0.88	0.77	0.91	0.79	0.95	0.96	0.92	49.55	11.47	34.22

The performance has been compared with an optimized standard 3D U-Net architecture to the network's performance, which has been tabulated in table 2.

Table 2: Performance of Regular 3D U-Net VS. Proposed Network

Dataset	Loss Function	Dice Score (%)		
		WT	CT	ET
Standard 3D U-Net	DL	72.5	12.44	0
	IOUL	59.89	9.35	0
	AW	67.22	16.34	0
Proposed NDNN	DL	91.43	88.10	82.06
	IOUL	87.29	86.80	84.65
	AW	89.36	87.4	86.33

The comparison made in table two shows that the proposed network performs better than the standard 3D U-Net even after parameter optimization. This comparison is illustrated in figure 10. It shows the proposed novel architecture outperforms standard 3D U-Net.

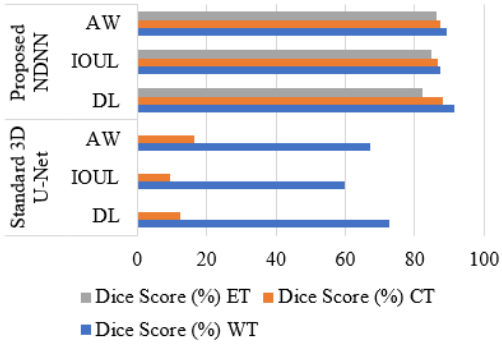

Figure 10: Performance comparison between proposed network and standard 3D U-Net with optimized parameters

The proposed network has been compared with five other papers to validate the performance further. The comparison has been listed in table 3

Table 3: Proposed paper VS. other similar papers on the same dataset

Dataset	Author	Dice Score (%)		
		WT	CT	ET
BraTS 2020	Lucas Fidon et al. [44]	88.9	84.1	84.1
	Théophraste Henry et al. [45]	79	89	84
	Fabian Isensee [46]	88.95	85.06	82.03
	Yixin Wang [47]	89.10	84.20	81.60
	Parvez Ahmad [48]	89.12	84.74	79.12
	Proposed	**90.02**	**85.11**	**84.41**

The proposed novel architecture to segment brain tumors performs better than regular 3D U-Net architecture. Moreover, the proposed methodology outperforms existing research. It has been observed dice score of CT of Théophraste Henry et al. is 3.89% higher than the proposed paper. However, the comparing paper suffers from poor performance in the WT region. Considering the overall performance, this paper's network architecture and innovative methodology perform better than existing solutions. The proposed NDNN-based U-net has experimented with BraTS 2015, 2016, 2017, and 2020 datasets. The training performance of the network on these datasets has been listed in table 4.

Table 4: Performance comparison of the proposed network on different datasets.

Method	Dataset	ET	WT	TC
Proposed Method	BraTS 2015	0.84	0.91	0.81
	BraTS 2016	0.84	0.92	0.81
	BraTS 2017	0.86	0.93	0.85
	BraTS 2020	0.85	0.94	0.84

The ribbon graph illustrated in figure 11, which represents the performance variation of the proposed network for different datasets, demonstrates the nominal differences among ET, WT, and TC. It proves negligible differences among the proposed network's performances for different datasets. The standard deviation in performance for ET, WT, and TC for different datasets are 0.0083, 0.011, and 0.018, respectively.

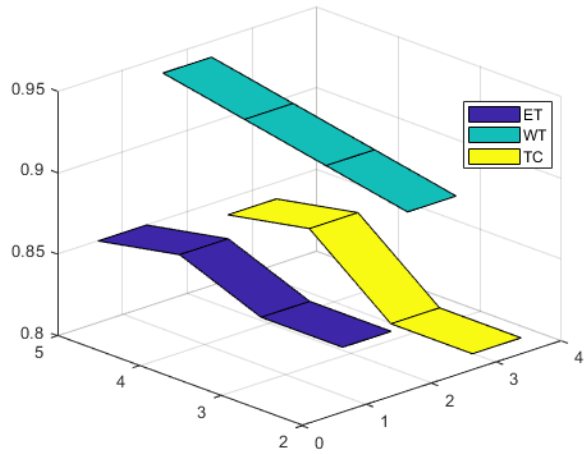

Figure 11: The performance variations for different datasets

The performance analysis based on the experimented results on multiple evaluation criteria and comparisons establishes the superiority of the proposed network in 3D brain tumor segmentation.

V. Conclusion and Discussion

The novel concept of using NDNN-based U-Net architecture paves the path to uplifting the performance of computer-aided automatic brain tumor segmentation to a new level. Although the complexity of the proposed network is much higher than existing researchers, the network's performance compensates for the computation complexity. 3D brain tumor segmentation, unlike 2D object segmentation, is a challenging and complicated task. Both shape, volume, and depth must be considered while working with 3D brain tumor segmentation. Moreover, the multimodalities in the MRI images include additional difficulties. This paper proposed and experimented with an efficient MFS Net to fuse the multimodalities into a single lossless modality. Then the single modality scans are used to train a nested network consisting of cNode, which paves the path to include multidimensional computation load in nodes of a deep neural network with the demonstration of better performance than existing solutions. Altogether, the proposed methodology contributes to the further develop the computer-aided automatic brain tumor segmentation process with a novel NDNN-based U-Net architecture that performs better than existing published literature.

References

[1] Sun, L., Zhang, S., Chen, H., & Luo, L. (2019). Brain tumor segmentation and survival prediction using multimodal MRI scans with deep learning. Frontiers in neuroscience, 13, 810.

[2] Gondal, A. H., & Khan, M. N. A. (2013). A review of fully automated techniques for brain tumor detection from MR images. International Journal of Modern Education and Computer Science, 5(2), 55.

[3] Zhou, Tongxue, Su Ruan, and Stéphane Canu. "A review: Deep learning for medical image segmentation using multimodality fusion." Array 3 (2019): 100004.

[4] Perez, Jaime, et al. "MRI and CT fusion in stereotactic electroencephalography: a literature review." Applied Sciences 11.12 (2021): 5524.

[5] Adelbratt, Susan, and Peter Strang. "Death anxiety in brain tumour patients and their spouses." Palliative medicine 14.6 (2000): 499-507.

[6] Trivedi, Mahendra Kumar, et al. "The potential impact of biofield treatment on human brain tumor cells: A time-lapse video microscopy." Integrative Oncology 4.3 (2015): 1000141.

[7] Eljamel, Sam. "Photodynamic applications in brain tumors: a comprehensive review of the literature." Photodiagnosis and photodynamic therapy 7.2 (2010): 76-85.

[8] Hu, An, and Navid Razmjooy. "Brain tumor diagnosis based on metaheuristics and deep learning." International Journal of Imaging Systems and Technology 31.2 (2021): 657-669.

[9] Suganyadevi, S., V. Seethalakshmi, and K. Balasamy. "A review on deep learning in medical image analysis." International Journal of Multimedia Information Retrieval 11.1 (2022): 19-38.

[10] Das, Suchismita, et al. "An artificial intelligence framework and its bias for brain tumor segmentation: A narrative review." Computers in Biology and Medicine (2022): 105273.

[11] Kim, Taeyun, et al. "Comparison of X-ray computed tomography and magnetic resonance imaging to detect pest-infested fruits: A pilot study." Nuclear Engineering and Technology 54.2 (2022): 514-522.

[12] Lundervold, Alexander Selvikvåg, and Arvid Lundervold. "An overview of deep learning in medical imaging focusing on MRI." Zeitschrift für Medizinische Physik 29.2 (2019): 102-127.

[13] Balwant, M. K. "A Review on Convolutional Neural Networks for Brain Tumor Segmentation: Methods, Datasets, Libraries, and Future Directions." IRBM (2022).

[14] Faruqui, Nuruzzaman, et al. "LungNet: A hybrid deep-CNN model for lung cancer diagnosis using CT and wearable sensor-based medical IoT data." Computers in Biology and Medicine 139 (2021): 104961.

[15] Verburg, Erik, et al. "Deep learning for automated triaging of 4581 breast MRI examinations from the DENSE trial." Radiology 302.1 (2022): 29-36.

[16] Sauter, A. W., Wehrl, H. F., Kolb, A., Judenhofer, M. S., & Pichler, B. J. (2010). Combined PET/MRI: one step further in multimodality imaging. Trends in molecular medicine, 16(11), 508-515.

[17] Kroon, Dirk-Jan, and Cornelis H. Slump. "MRI modalitiy transformation in demon registration." 2009 IEEE International Symposium on Biomedical Imaging: From Nano to Macro. IEEE, 2009.

[18] Lahat, Dana, Tülay Adalý, and Christian Jutten. "Challenges in multimodal data fusion." 2014 22nd European Signal Processing Conference (EUSIPCO). IEEE, 2014.

[19] Dalla Mura, Mauro, et al. "Challenges and opportunities of multimodality and data fusion in remote sensing." Proceedings of the IEEE 103.9 (2015): 1585-1601.

[20] Li, Jiaxin, et al. "Deep learning in multimodal remote sensing data fusion: A comprehensive review." arXiv preprint arXiv:2205.01380 (2022).

[21] Punn NS, Agarwal S (2020) Inception u-net architecture for semantic segmentation to identify nuclei in microscopy cell images. ACM Trans Multimed Comput Commun Appl (TOMM) 16(1):1–15.

[22] Mubashar, Mehreen, et al. "R2U++: a multiscale recurrent residual U-Net with dense skip connections for medical image segmentation." Neural Computing and Applications (2022): 1-17.

[23] Phan, Kim Ngan, et al. "Expression classification using concatenation of deep neural network for the 3rd abaw3 competition." arXiv preprint arXiv:2203.12899 (2022).

[24] Zhao, Xiaomei, et al. "A deep learning model integrating FCNNs and CRFs for brain tumor segmentation." Medical image analysis 43 (2018): 98-111.

[25] Mlynarski, Pawel, et al. "Deep learning with mixed supervision for brain tumor segmentation." Journal of Medical Imaging 6.3 (2019): 034002.

[26] Ottom, Mohammad Ashraf, Hanif Abdul Rahman, and Ivo D. Dinov. "Znet: Deep Learning Approach for 2D MRI Brain Tumor Segmentation." IEEE Journal of Translational Engineering in Health and Medicine (2022).

[27] B. H. Menze, A. Jakab, S. Bauer, J. Kalpathy-Cramer, K. Farahani, J. Kirby, et al. "The Multimodal Brain Tumor Image Segmentation Benchmark (BRATS)", IEEE Transactions on Medical Imaging 34(10), 1993-2024 (2015) DOI: 10.1109/TMI.2014.2377694

[28] S. Bakas, H. Akbari, A. Sotiras, M. Bilello, M. Rozycki, J.S. Kirby, et al., "Advancing The Cancer Genome Atlas glioma MRI collections with expert segmentation labels and radiomic features", Nature Scientific Data, 4:170117 (2017) DOI: 10.1038/sdata.2017.117

[29] S. Bakas, M. Reyes, A. Jakab, S. Bauer, M. Rempfler, A. Crimi, et al., "Identifying the Best Machine Learning Algorithms for Brain Tumor Segmentation, Progression Assessment, and Overall Survival Prediction in the BRATS Challenge", arXiv preprint arXiv:1811.02629 (2018)

[30] Liu, Yu, et al. "Multimodal MRI Volumetric Data Fusion with Convolutional Neural Networks." IEEE Transactions on Instrumentation and Measurement (2022).

[31] Montaha, Sidratul, et al. "TD-CNN-LSTM: A Hybrid approach combining CNN and LSTM to classify brain tumor on 3D MRI scans performing ablation study." IEEE Access (2022).

[32] Szegedy, Christian, et al. "Rethinking the inception architecture for computer vision." Proceedings of the IEEE conference on computer vision and pattern recognition. 2016.

[33] Agarap, Abien Fred. "Deep learning using rectified linear units (relu)." arXiv preprint arXiv:1803.08375 (2018).

[34] Siddique, Nahian, et al. "U-net and its variants for medical image segmentation: A review of theory and applications." Ieee Access 9 (2021): 82031-82057.

[35] Targ, Sasha, Diogo Almeida, and Kevin Lyman. "Resnet in resnet: Generalizing residual architectures." arXiv preprint arXiv:1603.08029 (2016).

[36] Ebrahimi, Mohammad Sadegh, and Hossein Karkeh Abadi. "Study of residual networks for image recognition." Intelligent Computing. Springer, Cham, 2021. 754-763.

[37] Srivastava, Nitish, et al. "Dropout: a simple way to prevent neural networks from overfitting." The journal of machine learning research 15.1 (2014): 1929-1958.

[38] Xu, Dongpo, et al. "Convergence of the RMSProp deep learning method with penalty for nonconvex optimization." Neural Networks 139 (2021): 17-23.

[39] Ma, Jerry, and Denis Yarats. "Quasi-hyperbolic momentum and Adam for deep learning." arXiv preprint arXiv:1810.06801 (2018).

[40] Wang, Feifan, et al. "3d u-net based brain tumor segmentation and survival days prediction." International MICCAI Brainlesion Workshop. Springer, Cham, 2019.

[41] Qin, Chuanbo, et al. "Improved U-Net3+ with stage residual for brain tumor segmentation." BMC Medical Imaging 22.1 (2022): 1-15.

[42] Hu, Jingyu, Xiaojing Gu, and Xingsheng Gu. "Mutual Ensemble Learning for Brain Tumor Segmentation." Neurocomputing (2022).

[43] Kotowski, Krzysztof, et al. "Coupling nnU-Nets with Expert Knowledge for Accurate Brain Tumor Segmentation from MRI." International MICCAI Brainlesion Workshop. Springer, Cham, 2022.

[44] Fidon, Lucas, Sébastien Ourselin, and Tom Vercauteren. "Generalized wasserstein dice score, distributionally robust deep learning, and ranger for brain tumor segmentation: BraTS 2020 challenge." International MICCAI Brainlesion Workshop. Springer, Cham, 2020.

[45] Henry, Theophraste, et al. "Brain tumor segmentation with self-ensembled, deeply-supervised 3D U-net neural networks: a BraTS 2020 challenge solution." International MICCAI Brainlesion Workshop. Springer, Cham, 2020.

[46] Isensee, Fabian, et al. "nnU-Net for brain tumor segmentation." International MICCAI Brainlesion Workshop. Springer, Cham, 2020.

[47] Wang, Yixin, et al. "Modality-pairing learning for brain tumor segmentation." International MICCAI Brainlesion Workshop. Springer, Cham, 2020.

[48] Ahmad, Parvez, et al. "Context aware 3D UNet for brain tumor segmentation." International MICCAI Brainlesion Workshop. Springer, Cham, 2020.

View publication stats